Journal of Food Engineering xxx (2010) xxx–xxx

Contents lists available at ScienceDirect

Journal of Food Engineering

journal homepage: www.elsevier.com/locate/jfoodeng

Structure and properties of nanocomposite films based on sodium caseinate and nanocellulose fibers

Mariana Pereda [a], Guillermina Amica [a], Ilona Rácz [b], Norma E. Marcovich [a,*]

[a] INTEMA (Univ. Nacional de Mar del Plata, CONICET), Juan B. Justo 4302, 7600 Mar del Plata, Argentina
[b] Bay Zoltán Foundation for Applied Research, Institute for Materials Science and Technology, H-1116 Budapest, Fehérvári 130, Hungary

ARTICLE INFO

Article history:
Received 22 July 2010
Received in revised form 27 September 2010
Accepted 2 October 2010
Available online xxxx

Keywords:
Nanocellulose fibers
Sodium caseinate
Biopolymers
Proteins
Nanocomposites

ABSTRACT

Films made from sodium caseinate and nanocellulose were prepared by dispersing the fibrils into film forming solutions, casting and drying. Composite films were less transparent and had a more hydrophilic surface than neat sodium caseinate ones. However, the global moisture uptake was almost not affected by filler concentration. Addition of nanocellulose to the neat sodium caseinate films produced an initial increase in the barrier properties to water vapor, and then, it decreases as filler content increased. This was explained in terms of additional detrimental changes (cracks and bubble formation) induced in the morphological structure of the film by the reinforcement.

The tensile modulus and strength of composite films increased significantly with increasing cellulose concentrations, while the values of elongation decreased. In the same way it was found that the storage modulus increases considerably with filler addition in the low temperature range (<60 °C), though the effect of temperature on the films performance is even more dramatic, as expected in protein-based materials.

1. Introduction

Nowadays, most materials used for food packaging are practically non-degradable, representing a serious global environmental problem. Accordingly, edible films based on natural materials are receiving much attention as potential packaging materials, principally because such biodegradable films are considered to be a promising solution to environmental impacts of synthetic polymer packaging (Wang et al., 2008; Su et al., 2010). The production of biodegradable and edible films from carbohydrates and proteins adds value to low cost raw materials and can play an important role in food preservation by extending shelf life and improving quality of foods (Avérous et al., 2001; Gennadios, 2002; Krochta and Miller, 1997; Tharanathan, 2003). Preparing these films involves the use of at least one film-forming agent (macromolecule), a solvent and a plasticizer.

However, biopolymer films are limited in their ability to obtain wide commercial application due to disadvantages related to performance (such as brittleness, poor gas and moisture barrier), processing (such as low heat distortion temperature), and cost. Although plasticizers are generally added into film-forming solutions to prevent film brittleness or cracking caused by intermolecular forces (Lieberman and Gilbert, 1973; Sothornvit and Krochta, 2001; Ibrahim et al., 2010), the weakness of biopolymer films in mechanical properties may not be easily overcome.

Over the past decades, interest in sustainability and green chemistry has lead to a renewed interest in novel cellulosic materials (Ragauskas et al., 2006; Ibrahim et al., 2010) and composites (degree Well et al., 2004) derived from a variety of cellulosics (Samir et al., 2005; Ibrahim et al., 2010). Cellulose, which is a natural polysaccharide, is one of the most abundant materials in the natural world, and its biosynthesis, chemistry, and ultra structure remain as active fields of study (Klem et al., 2005; Klemm et al., 2002). In the same way, cellulose fibers with one nano/micro scale dimension are attractive as reinforcing fillers in polymeric matrices due to their good mechanical properties with very high bending strength and stiffness (e.g. Young's modulus of about 150 GPa (Cao et al., 2007)). Because of their size, nanoparticles have proportionally larger surface area and consequently more surface atoms than their microscale counterpart. In the nanoscale range, materials may present different electronic properties, which in turn affects its optical, catalytic and other reactive properties (Boccuni et al., 2008; Kahn, 2006). Moreover, macroscopic reinforcing fillers usually contain defects, which become less important as the particle size become smaller (Ludueña et al., 2007). In addition to the effects of the nanoreinforcements themselves, an interphase region of altered mobility surrounding each nanoparticle is induced by well dispersed nanoparticles, resulting in a percolating interphase network in the composite and playing an important role in improving the nanocomposite properties (Qiao and Brinson, 2009; Azeredo, 2009). According to Jordan et al. (2005), for any constant filler content, a reduction in particle size increases the

* Corresponding author. Tel.: +54 223 481 6600; fax: +54 223 481 0046.
E-mail address: marcovic@fi.mdp.edu.ar (N.E. Marcovich).

0260-8774/$ - see front matter © 2010 Elsevier Ltd. All rights reserved.
doi:10.1016/j.jfoodeng.2010.10.001

number of filler particles, bringing them closer to one another; thus, the interface layers from adjacent particles overlap, altering the bulk properties significantly. Summarizing, the advantages of nanocomposite materials, compared with conventional composites, are their superior thermal, mechanical and barrier properties even at very low reinforcement content (<5 wt%), added to a better recyclability and low weight (Oksman et al., 2006). In this perspective, it is interesting to study the behavior of nanocomposites based on natural resources, as Oksman et al. (2006) did. They used cellulose whiskers and polylactic acid to develop nanostructured composites by compounding extrusion with enhanced properties. Psomiadou et al. (1996) worked on extruded and hot pressed edible films prepared from starch and microcrystalline cellulose (MCC)/methylcellulose (MC) and reported increased elongation and strength added to lower water permeation values for samples prepared with relatively high MCC or MC contents. Su et al. (2010) developed edible films based on carboxymethyl cellulose (CMC) and soy protein isolate (SPI) and found that CMC and SPI formed one phase blends. Moreover, increasing the CMC content improved the mechanical properties and reduced the water sensitivity of blend films. Ibrahim et al. (2010) developed reinforced films from polyvinyl alcohol and nanospherical cellulose that showed increased tensile strength and elongation at break at 20% load. However and as far as we know, most of the work in this area was concentrated in biopolymers different than those derived from proteins (Müller and Borges Laurindo, 2009; Müller et al., 2009; Chang et al., 2010; Ibrahim et al., 2010; Oksman et al., 2006; Psomiadou et al., 1996) or the interests were different, i.e. producing blends using cellulose derivatives and proteins to study adsorption characteristics (Pérez et al., 2009). Thus, the focus of this work is to prepare and characterize films based on glycerol-plasticized sodium caseinate (SC) and nanocellulose (NC) fibers made by casting of aqueous suspensions.

2. Experimental

2.1. Materials and methods

2.1.1. Materials

Sodium caseinate (SC) powder, containing 88.9 wt% protein (the rest being lactose, lipids, attached moisture, and ashes), was obtained from Lactoprot Deutschland GmbH (Germany). The average protein molecular weight is 22,600 g mol^{-1} (Audic and Chaufer, 2005). The plasticizer used was glycerol (GLY) P.A., which was purchased from DEM Chemicals (Mar del Plata, Argentina). Microcrystalline cellulose powder (MCC) of 20 μm (Aldrich, Cat. No. 31,069-7) was selected as the source raw material for producing the cellulose crystals.

2.1.2. Swelling and separation of microcrystalline cellulose

The microcrystalline cellulose was swelled and partly separated to whiskers by chemical and ultra sonification treatments according the procedure proposed by Oksman et al. (2006). A *N*,*N*-dimethyl acetamide with 0.5% LiCl solution was used as swelling medium. Microcrystalline cellulose was added to the swelling solution (10 wt%) and agitated using a magnetic stirrer for 12 h at 70 °C. Then, the slightly swelled particles were sonified in an ultrasonic bath for 3 h over a period of 5 days with long intervals between each sonification treatment, to separate cellulose nano whiskers. The gel-like suspension was repeatedly washed with distilled water and then freeze-dried.

2.1.3. Film preparation

Sodium caseinate aqueous solutions with protein concentrations of 2.5% (w/v) were prepared by dissolving the sodium caseinate powder in distilled water and stirring continuously for 3 h at room temperature. Appropriate amount of glycerol was added to achieve a glycerol/(sodium caseinate + glicerol) weight ratio of 0.21. Nanocellulose fibers were dispersed in distilled water by ultrasonication and then mixed with the film forming solutions to prepare composites containing 1, 2 and 3 wt% cellulose (dry weight). Films were prepared according to the usual casting method: the solutions were poured into Teflon Petri dishes (diameter = 14 cm) and dried at 35 °C for approximately 10 h in a convection oven. After the excess of water was evaporated, the obtained films were peeled off from the plates and kept in a closed reservoir at 50% relative humidity (RH) and constant temperature (23 ± 2 °C) for 3 days.

2.2. Characterization of the films

2.2.1. Infrared spectroscopy

FTIR spectra of the films were recorded using the attenuated total reflection method (ATR) in a Genesis II (Mattson) Fourier transform infrared spectrometer. On the other hand, nanocellulose was examined by DRIFT (diffuse reflectance FTIR). In both cases, the spectra were recorded over a range of 600–4000 cm^{-1} with a resolution of 2 cm^{-1} and averaged over 32 scans.

2.2.2. Opacity

Film opacity was determined according to the method described by Irissin-Mangata et al. (2001) on rectangular strips directly placed in a UV–Visible spectrophotometer test cell. The absorption spectrum of the sample was obtained from 400 to 800 nm in a UV–Visible spectrophotometer Shimadzu 1601 PC (Tokyo, Japan). Film opacity was defined as the area under the curve divided by film thickness and expressed as Absorbance Units × nanometers/millimeters (AU nm/mm). Measurements were taken in triplicate for each sample.

2.2.3. Water vapor permeability (WVP)

The water vapor transfer rate [g/s m^{-2}] through films was determined gravimetrically using the ASTM Method E96-95 (ASTM, 1995). Prior to the test, the films were placed in a chamber maintained at room temperature for 3 days at 64.5% RH, to ensure equilibrium conditions. After that, film specimens were sealed on acrylic permeation cups (5 cm diameter) containing water (100% RH). The cups were weighed at 1 h intervals over a 6 h period. A fan located inside the chamber was used to move the internal air ensuring uniform conditions at all test locations. Linear regression was used to fit the data, weight vs. time, and to calculate the slope of the resulting straight line in g s^{-1}. WVP of the films, expressed as [g m/(Pa s m^2)], was calculated as follows:

$$\mathrm{WVP} = \Delta W y [A \Delta t (p_2 - p_1)]^{-1} \quad (1)$$

where ΔW is the weight of water absorbed in the cup (g), Δt the time for weight change (thus $\Delta W/\Delta t$ is the slope calculated from a plot of cup weight vs. time), A is the exposed area of the film (m^2), y is the film thickness (m), and $p_2 - p_1$ is the vapor pressure difference across the film (Pa), which was calculated based on the chamber temperature and the relative humidity inside and outside the cup. Four specimens were tested for each cellulose concentration.

2.2.4. Surface hydrophobicity (contact angle)

The surface hydrophobicity of the films was estimated by the sessile drop method, based on optical contact angle method. Contact angle measurements were carried out with a homemade instrument. A droplet of ethylene–glycol (Aldrich Co.) (5 μL) was deposited on the film surface with an automatic piston syringe. The drop image was photographed using a digital camera. An

Please cite this article in press as: Pereda, M., et al. Structure and properties of nanocomposite films based on sodium caseinate and nanocellulose fibers. Journal of Food Engineering (2010), doi:10.1016/j.jfoodeng.2010.10.001

image analyzer was used to measure the angle formed between the surface of the film in contact with the drop, and the tangent to the drop of liquid at the point of contact with the film surface. Seven replicate measurements were performed for each film at 24 °C, with a precision of ±2 °C.

2.2.5. Moisture sorption

The films, dried at 40 °C for three days in a vacuum oven, were placed into an environmental chamber maintained at 75% relative humidity (RH) and 23 ± 2 °C, to obtain water sorption isotherms. Samples were taken out of the chamber at regular time intervals and weighed with a precision of ±0.0001 g. The moisture content (M_t) of the films as a function of time was obtained from the total mass balance over the sample, as follows:

$$M_t = \frac{(W_t - W_0)}{W_0} \cdot 100 \quad (2)$$

where M_t is the moisture content of the sample at a fixed time expressed in dry basis [%]; W_t is the weight of the sample at a fixed time [g] and W_0 is the initial dry weight of the sample [g]. The curves were fitted according to the Fick's diffusion equation for the unidimensional diffusion of a solute into a sheet (Crank, 1956):

$$\frac{M_t}{M_\infty} = 1 - \frac{8}{\pi^2}\sum_{n=0}^{\infty}\frac{1}{(2n+1)^2}\exp\left[-D\frac{(2n+1)^2\pi^2 t}{l^2}\right] \quad (3)$$

where M_∞ is the amount of water absorbed at equilibrium, D is the effective diffusion coefficient, t is the time and l is the average thickness of the film. To ensure the reproducibility of the results, four specimens for each sample were tested.

2.2.6. Tensile

Tensile tests were performed at room temperature (23 ± 2 °C) using an Instron Universal Testing Machine model 8501. The specimens were cut according to the ASTM D1708-93 (ASTM, 1993). Five specimens from each film were tested from a minimum of three films per sample. Crosshead speed was set at 10 mm/min. The ultimate strength (σ_b), elongation at break (ε_b) and elastic modulus (E) were calculated as described in ASTM D638-94b (ASTM, 1994).

2.2.7. Dynamic-mechanical analysis

The thermo-mechanical response of specific samples was determined using a rheometer (Anton Paar, Physica MCR 301) in torsion mode. Tests were conducted using the temperature scan mode, applying a deformation of 0.05%. The frequency of the forced oscillations was fixed at 1 Hz. The specimens were cut to 40 × 10 mm, and the dimensions were measured with an accuracy of 0.01 mm.

2.2.8. Scanning electron microscopy (SEM)

The fracture surfaces (transversal area) obtained after immersing film samples in liquid air (fragile fracture) as well as the main surfaces of the films (upper and lower) were observed using a scanning electron microscope (JEOL, model JSM-6460 LV). For this purpose, selected pieces of the films were mounted on bronze stubs using a double-sided tape and then coated with gold, before being observed under the microscope.

2.2.9. Porosity measurements

The Image-Pro Plus 4.5 software was used to determine the percentage of the film surface that corresponds to pores and voids. Five SEM images obtained from the upper surface of each film sample at 1000× magnification were analyzed (total area 66,320 μm^2).

2.2.10. Statistical analysis

Data for each test were statistically analyzed. The analysis of variance (ANOVA) was used to evaluate the significance in the difference between factors and levels. Comparison of the means was done employing a Tukey test to identify which groups were significantly different from other groups ($P < 0.05$). All data are presented as mean ± SD.

3. Results and discussion

3.1. Physical characterization

Fig. 1 shows the FTIR spectra of the films prepared without and with 3 wt% cellulose together with the spectrum of the neat nanocellulose. The changes introduced by the addition of cellulose to sodium caseinate films are minor, as expected from the low amount of filler used to make the composite films. In fact, only a closer examination reveals a minimum increase in the peaks at 1040, 1110 and 1640 cm^{-1} in the 3% film respect to the unreinforced one. The peak at 1040 cm^{-1} can be attributed to the C–O stretching in cellulose, while the contribution at 1100 cm^{-1} corresponds to the skeletal vibration involving C–O stretching of the β(1 → 4) glycosidic linkages of the β-D-glucopyranosyl units of cellulose (Marcovich et al., 1996). Regarding the band at 1690–1590 cm^{-1}, it corresponds to the amide I vibrations (common to proteins, Pereda et al., 2008) and also to adsorbed water molecules in noncrystalline cellulose (Jayaramudu et al., 2009). Moreover, the existence of this band in the spectrum of neat cellulose confirms that it is highly but not 100% crystalline.

Transparency of films designed for packaging is a relevant property since it has a direct impact on the appearance of the coated product. The opacity is an established measurement of the transparency of a film: a greater value of opacity means a smaller transparency (Cuq et al., 1996; Casariego et al., 2009). Table 1 shows the opacity values as a function of the nanocellulose content. It is clear that the films are less transparent as the filler content increases. The presence of a disperse phase promotes opacity as a function of the differences in the refractive index of both phases and the concentration and particle size of the filler (Villalobos et al., 2005). The increase in film opacity arises from the light scattering produced by the cellulose particles thoroughly distributed in the

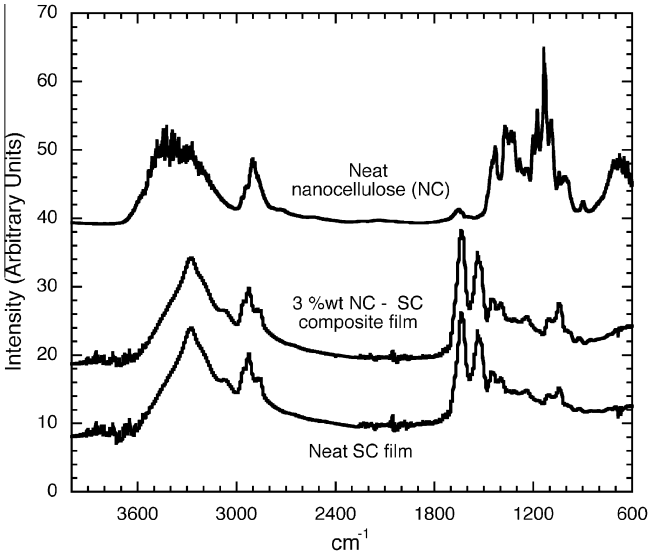

Fig. 1. FTIR spectra of sodium caseinate film, 3% nanocellulose reinforced caseinate film and neat nanocellulose.

Please cite this article in press as: Pereda, M., et al. Structure and properties of nanocomposite films based on sodium caseinate and nanocellulose fibers. Journal of Food Engineering (2010), doi:10.1016/j.jfoodeng.2010.10.001

Table 1
Opacity and contact angle values of sodium caseinate films reinforced with nanocellulose.

Nanocellulose (wt%)	Opacity (AU nm/mm)	θ (°)
0	1461.9 ± 35.9[a]	40.2 ± 2.2[a]
1	2137.7 ± 434.0[b]	32.8 ± 4.2[b]
2	2275.3 ± 451.2[b]	29.7 ± 2.7[b]
3	3215.2 ± 214.9[c]	29.7 ± 1.5[b]

[a–c] Different superscripts within the same column indicate significant differences between formulations ($P < 0.05$).

protein network that constitutes the film, reducing the overall light transmitted through it. These observations are consistent with the finding of different researchers in related systems such as films prepared from protein–lipid emulsions (Monedero et al., 2009; Yang and Paulson, 2000; Prodpran et al., 2007) or reinforced by nanoclays (Tunç and Duman, 2010). Moreover, while the addition of very low amounts of filler produces a moderate increase in the opacity values in comparison with the corresponding to the neat protein film (55% for 2 wt%), the incorporation of only 3 wt% lead to a marked opacity (120% increase), which could be associated to a percolated system (nanofibers spanning the whole sample).

The contact angles (using ethylene–glycol as polar solvent) of the different films are also reported in Table 1. It is clear that cellulose addition causes an increase in the superficial hydrophilicity of the reinforced samples with respect to the neat caseinate one, although there are no important differences with filler concentration. Component rearrangement in the film matrix during the film drying, which defines its internal and surface structure, has an important role in surface properties. During the film forming process the hydrophobic parts of protein were mainly turned towards film–air and film–plate interfaces, while hydrophilic parts were mainly turned towards internal parts (Villalobos et al., 2005; Pérez et al., 2009), thus, the global hydrophicity is different from the surface one in protein films. However, the very polar cellulose nanofibers do not have the caseinate amphiphilic chemical characteristics and consequently they lead to an increase in the surface hydrophilicity of the composite films.

3.2. Water vapor permeability and moisture sorption

A motivating factor in developing nanocomposite from sodium caseinate films is to improve barrier properties. Moisture barrier of polymer films has been improved by nanocellulose addition (Azeredo, 2009; Paralikar et al., 2008; Sanchez-Garcia et al., 2008; Svagan et al., 2009). The presence of crystalline fibers is thought to increase the tortuosity in the materials leading to slower diffusion processes and, hence, to lower permeability (Sanchez-Garcia et al., 2008; Casariego et al., 2009). The barrier properties are enhanced if the filler is less permeable, and have good dispersion in the matrix and a high aspect ratio (Lagaron et al., 2004). However, permeability also depends on membrane porosity, surface absorption and desorption behavior of the permeant, relative humidity, and the amount of plasticizer used (Kim, 2005; Park, 1991). Fig. 2 shows that the addition of nanocellulose to the neat sodium caseinate films produces an initial increase in the barrier properties to water vapor, and then, the permeability decreases as filler content increases. To understand this behavior, the morphology of the reinforced films was investigated using SEM. Fig. 3 shows the cryogenic fractured cross-section of selected films. It is clear that nanocellulose addition causes severe changes in the film microstructure, since the non-reinforced films exhibit a smooth, almost completely featureless surface, as expected for a homogeneous material. On the contrary, even the addition of a small amount of

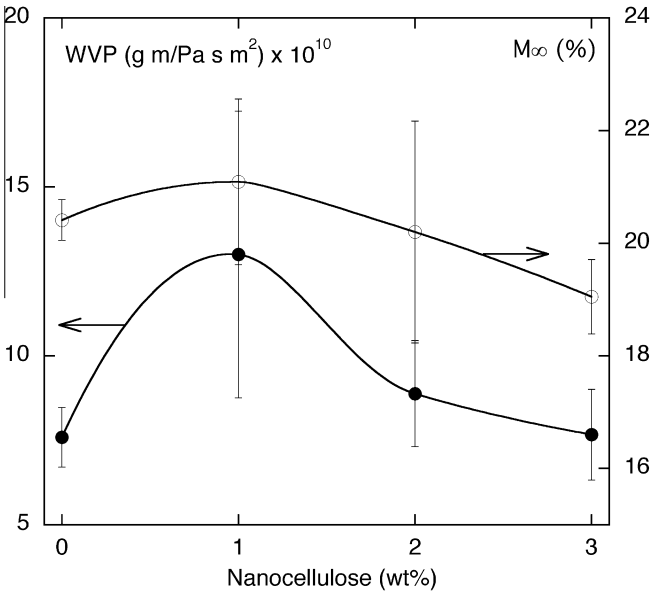

Fig. 2. Water vapor permeability and equilibrium moisture uptake of sodium caseinate films reinforced with nanocellulose.

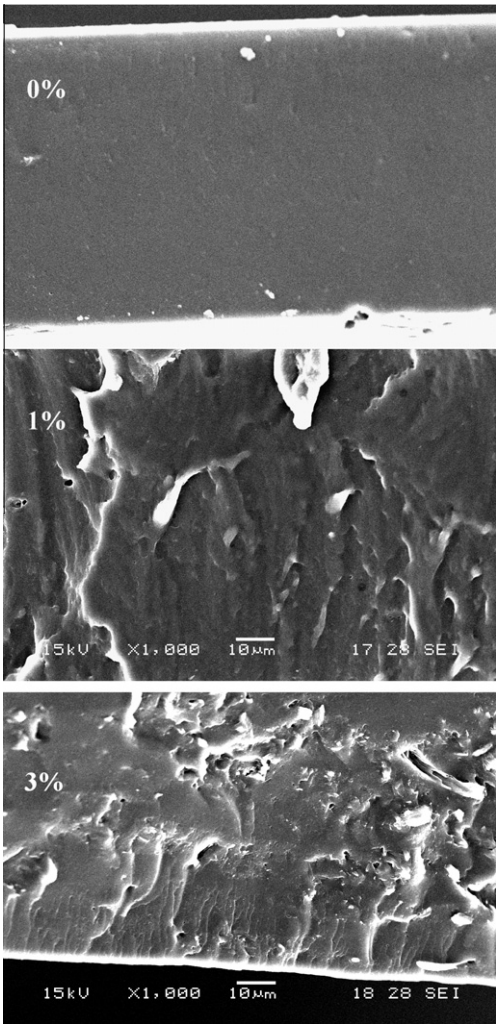

Fig. 3. Scanning electronic microscopies (transversal section) of the cryo-fractured nanocellulose reinforced caseinate films.

Please cite this article in press as: Pereda, M., et al. Structure and properties of nanocomposite films based on sodium caseinate and nanocellulose fibers. Journal of Food Engineering (2010), doi:10.1016/j.jfoodeng.2010.10.001

filler leads to a rough surface, with increasing density of crack deflection sites that results in increasing amount of ripples and ridges as cellulose concentration increases. During the cryogenic fracture of the reinforced films, the advancing crack must change path (deflection) because of the rigid filler, as observed by other researchers (Marcovich et al., 2006). On the other hand, Fig. 4 shows the appearance of the films surfaces. In all cases, some porous or bubbles, probably formed during the drying process due to trapped air are noticed. Nevertheless, the pore size and number increases with filler concentration, as presented in Table 2, probably because nanoparticles (although not seen at this magnification) acted as nucleating sites for bubble growing. Thus, the WVP of the reinforced films is determined by two opposite factors: the detrimental changes in the morphological structure and the increasing path length for vapor diffusion, in both cases compared to those of the neat protein film. It is clear that at least 3% cellulose addition is necessary to compensate the pore formation, recovering the WVP values of the neat matrix.

In the same way, it was reported that the water uptake of hydrophilic films (like starch ones) decreases linearly (Dufresne and Vignon, 1998; Dufresne et al., 2000) or almost linearly (Lu et al., 2005) with increasing cellulose whisker content. However, these authors used higher concentrations of cellulose fibrils (up to 40 wt%) and also admitted that starch was more hydrophilic than cellulose. In our case, the equilibrium moisture content of all samples differs only marginally, as shown in Fig. 2. Water sorption characteristics depend on the nature of all the constituents, filler, plasticizer and protein. Thus, being all of them mostly hydrophilic, a reduction in the water absorption capacity with cellulose addition was not expected. In contrast, the effective diffusion coefficient (Fig. 5) increases significantly with cellulose loads, which would indicate that plasticized caseinate is more hygroscopic than cellulose crystals. In this sense, the polar groups existent in the chemical structure of the protein represent a potential energy "sink" that can attract and bind water molecules. Consequently, the hydrogen bonding becomes a limiting factor in the diffusion

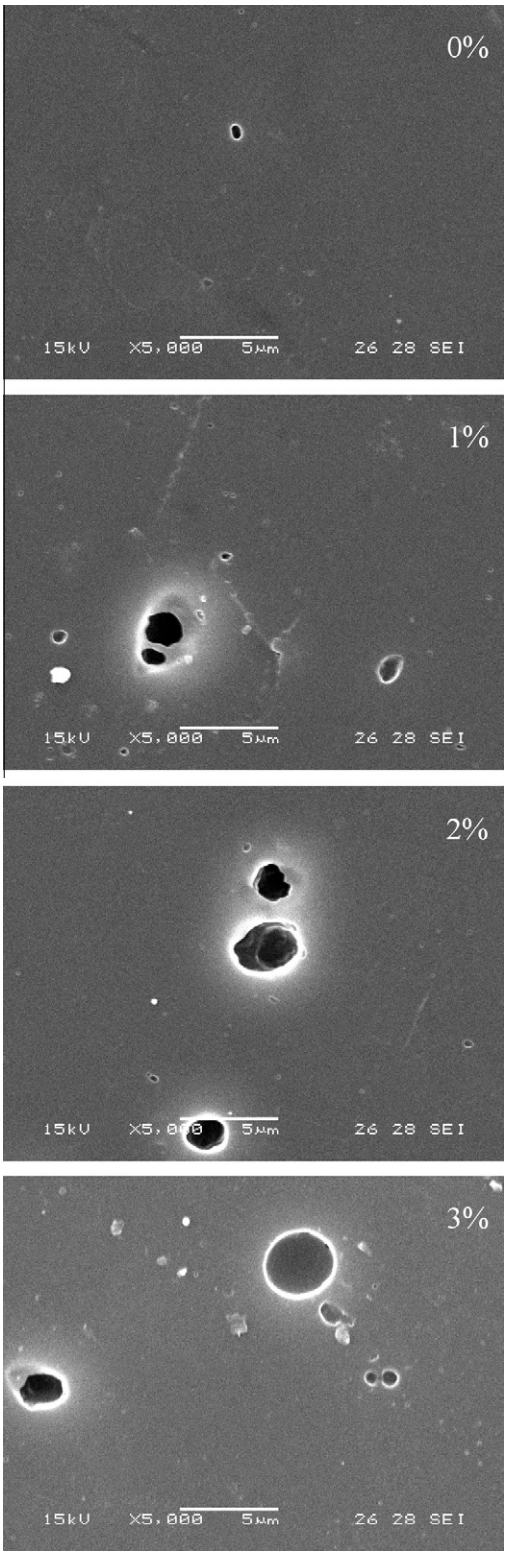

Fig. 4. Scanning electronic microscopies (upper surface) of nanocellulose reinforced caseinate films.

Table 2
Porosity measurements of sodium caseinate films reinforced with nanocellulose.

Nanocellulose (wt%)	Average porosity (%)	Pore area (μm^2)
0	0.108	0.85 ± 0.66[a]
1	0.116	0.96 ± 1.23[a]
2	0.160	1.09 ± 0.92[a]
3	0.194	1.24 ± 1.03[a]

[a–c] Different superscripts within the same column indicate significant differences between formulations ($P < 0.05$).

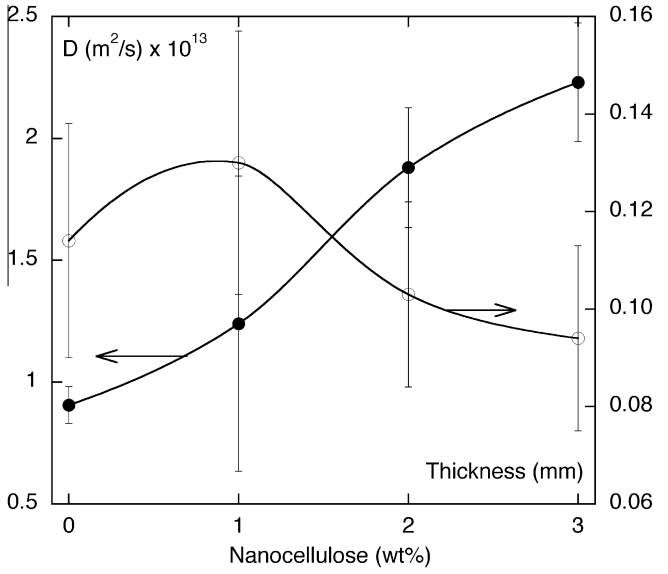

Fig. 5. Effective diffusion coefficient and average thickness of sodium caseinate films reinforced with nanocellulose.

Please cite this article in press as: Pereda, M., et al. Structure and properties of nanocomposite films based on sodium caseinate and nanocellulose fibers. Journal of Food Engineering (2010), doi:10.1016/j.jfoodeng.2010.10.001

of water vapor molecules into protein film that leads to the immobilization of the diffusing specie and contributes to delay its transport (Marcovich et al., 1999; Pereda et al., 2009). Moreover, this behavior could also denote a good dispersion of the filler in the matrix: since micro crystalline cellulose is prepared by removing part of the amorphous regions by acid degradation leaving the less accessible crystalline regions as fine crystals (Petersson and Oksman, 2006; Azeredo, 2009), it is expected that the swelled whiskers used in this work were mostly impermeable (Liu et al., 2010) crystalline fibers, not involved in binding water molecules. Thus, the important change of the diffusion coefficient with the low amounts of cellulose fibers used only can be explained considering that the filler exposed area is very large (well dispersed nanocrystals), covering the whole film surface.

3.3. Mechanical behavior

Fillers with a high ratio of the largest to the smallest dimension (i.e. aspect ratio) are particularly interesting because of their high specific surface area, providing better reinforcing effects (Azizi Samir et al., 2005; Dalmas et al., 2007; Dubief et al., 1999). This is the case in the present work; the addition of only 3%wt fibers produces more than a twofold increase in the tensile modulus of the composites, compared to the neat caseinate film, as noticed from Fig. 6. As can be observed from Fig. 7, the strength also increases indicating that the filler is properly dispersed in the matrix structure and also due to similarity between the chemical structures of cellulose and caseinate, as other authors noticed (Müller et al., 2009; Chang et al., 2010). On the other hand, the deformation at break decreases as cellulose concentration increases (Fig. 7), due to the rigid nature of the filler and again in agreement with previous results published in the literature (Curvelo et al., 2001; Müller and Borges Laurindo, 2009; Chang et al., 2010).

Finally, dynamic mechanical tests were carried out in an attempt to determine the effect of the filler on the glass–rubber transition temperature (T_g). Fig. 8 shows, quite clearly, that the storage modulus increases considerably with filler addition in the low temperature range. However, the effect of temperature on the film performance is even more dramatic, as expected in protein-based materials. As temperature increases, the samples become softer and finally reach the flow region. It is also clear that the temperature for entering in the flow zone, which can be considered as an indication of T_g, increases slightly with cellulose concentration.

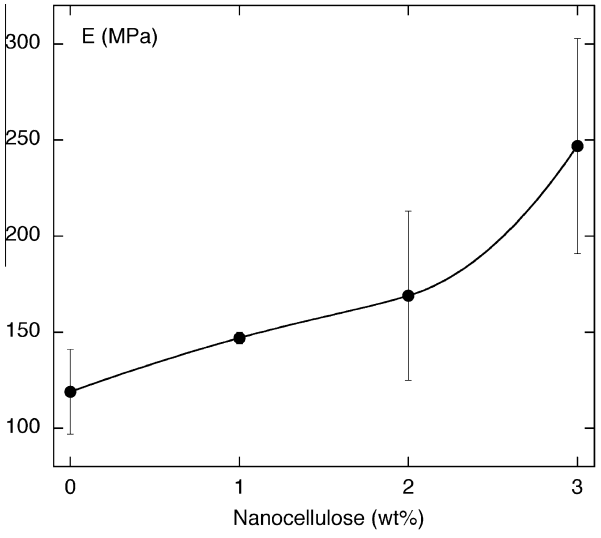

Fig. 6. Young modulus of sodium caseinate films reinforced with nanocellulose.

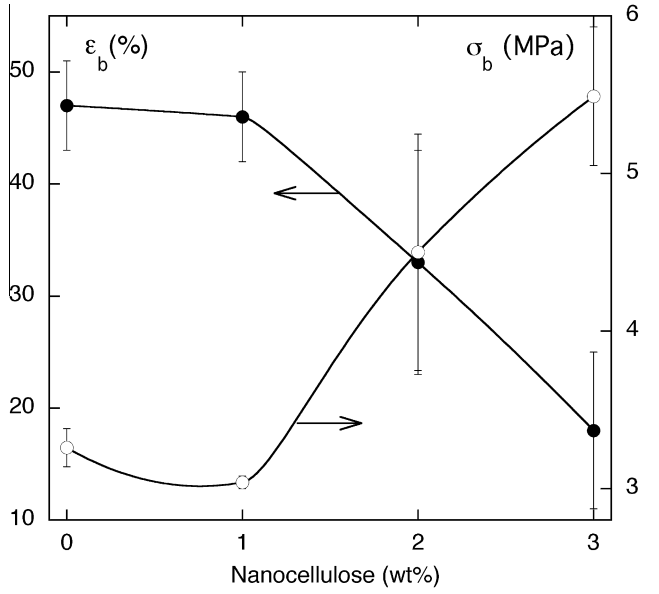

Fig. 7. Tensile strength and ultimate strain of sodium caseinate films reinforced with nanocellulose.

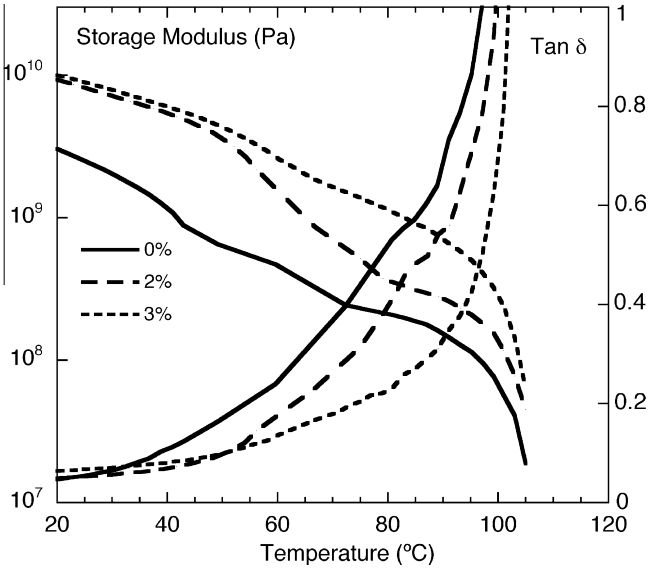

Fig. 8. Dynamic mechanical behavior of reinforced caseinate films.

Nanosized cellulose fibrils have been reported to improve thermal properties of polymers, although their effects on T_g of polymers have been controversial (Azeredo, 2009). Some authors reported T_g increasing effects on polymer films (Anglès and Dufresne, 2000; Dufresne and Vignon, 1998) but in other studies the effect of cellulose nanoreinforcements on T_g was not consistent (Azizi Samir et al., 2004; Mathew and Dufresne, 2002) or even negligible (Azizi Samir et al., 2004). Regarding the possible reasons for this behavior, one of the mechanisms proposed by Azizi Samir et al. (2004) can be used to explain our findings: the solid surface of cellulose whiskers could restrict mobility of polymer chains in the vicinity of the interfacial area, which would result in a global shift of T_g toward higher temperatures. In any case, it should be noticed that not only the moisture content of the films is decreasing as the test progress but also that cross-linkage in sodium caseinate films can be induced simply by heating (Pereda et al., 2010). In other

Please cite this article in press as: Pereda, M., et al. Structure and properties of nanocomposite films based on sodium caseinate and nanocellulose fibers. Journal of Food Engineering (2010), doi:10.1016/j.jfoodeng.2010.10.001

words, the "softening" temperature of the samples is changing as the test advances and cannot be ascribed to the standard T_g.

4. Conclusions

Composites made from glycerol-plasticized sodium caseinate and nanocellulose whiskers were prepared by casting of aqueous suspensions. Infrared spectroscopy revealed only minor changes attributed to cellulose addition due to the low amount of filler used to prepare the composite films.

The opacity increased and the contact angle using ethylene–glycol as polar solvent decreased with nanocellulose incorporation, thus, composite films are less transparent and have a more hydrophilic surface than neat sodium caseinate ones. However, the global moisture uptake is almost not affected by filler concentration. On the other hand, the addition of nanocellulose to the neat sodium caseinate films produced an initial increase in the water vapor permeability but then, it decreases as filler content increased. This was attributed to the contributions of two opposite factors: the increase in bubbles and pores content that affect the microstructure of the samples added to the increased path length for vapor diffusion with respect to the unreinforced caseinate samples.

The tensile modulus and strength of composite films increased significantly with increasing cellulose concentration, while the elongation decreased. In the same way the storage modulus increases considerably with filler addition in the low temperature range (<60 °C), although the effect of temperature on the films thermo-mechanical response is even more dramatic.

Acknowledgements

Authors thank the Ministry of Science, Technology and Productive Innovation (MINCYT) of Argentina (Project Number HU/07/07) and the National Office of Research and Technology (NKTH) of Hungary (Project Number TéT AR-7/2007) for the financial support.

References

Anglès, M.N., Dufresne, A., 2000. Plasticized starch/tunicin whiskers nanocomposites. 1. Structural analysis. Macromolecules 33, 8344–8353.
ASTM, 1993. Standard test method for tensile properties of Plastics by use of microtensile specimens, D1708-93. In: Annual Book of ASTM. Philadelphia, PA: American Society for Testing and Materials.
ASTM, 1994. Standard test method for tensile properties of Plastics, D638-94b. In: Annual Book of ASTM. Philadelphia, PA: American Society for Testing and Materials.
ASTM, 1995. Standard test methods for water vapor transmission of materials, E96-95. In: Annual Book of ASTM. Philadelphia, PA: American Society for Testing and Materials.
Audic, J.-L., Chaufer, B., 2005. Influence of plasticizers and crosslinking on the properties of biodegradable films made from sodium caseinate. European Polymer Journal 41, 1934–1942.
Avérous, L., Fringant, C., Moro, L., 2001. Plasticized starch–cellulose interactions in polysaccharides composites. Polymer 42, 6565–6572.
Azeredo, H.M.C., 2009. Nanocomposites for food packaging applications. Food Research International 42, 1240–1253.
Azizi Samir, M.A.S., Alloin, F., Sanchez, J.Y., Dufresne, A., 2004. Cellulose nanocrystals reinforced poly(oxyethylene). Polymer 45, 4149–4157.
Azizi Samir, M.A.S., Alloin, F., Dufresne, A., 2005. Review of recent research into cellulosic whiskers, their properties and their application in nanocomposite field. Biomacromolecules 6, 612–626.
Boccuni, F., Rondinone, B., Petyx, C., Iavicoli, S., 2008. Potential occupational exposure to manufactured nanoparticles in Italy. Journal of Cleaner Production 16, 949–956.
Cao, X.D., Dong, H., Li, C.M., 2007. New nanocomposite materials reinforced with flax cellulose nanocrystals in waterborne polyurethane. Biomacromolecules 8, 899–904.
Casariego, A., Souza, B.W.S., Cerqueira, M.A., Teixeira, J.A., Cruz, L., Díaz, R., Vicente, A.A., 2009. Chitosan/clay films' properties as affected by biopolymer and clay micro/nanoparticles' concentrations. Food Hydrocolloids 23, 1895–1902.
Chang, P.R., Jian, R., Yu, J., Ma, X., 2010. Fabrication and characterisation of chitosan nanoparticles/plasticised-starch composites. Food Chemistry 120, 736–740.
Crank, J., 1956. The Mathematics of Diffusion, first ed. Clarendon, Oxford.
Cuq, B., Gontard, N., Cuq, J.L., Guilber, S., 1996. Functional properties of myofibrillar protein based biopackaging as affected by film thickness. Journal of Food Science 61 (3), 580–584.
Curvelo, A.A.S., Carvalho, A.J.F., Agnelli, J.A.M., 2001. Thermoplastic starch-cellulosic fibers composites: preliminary results. Carbohydrate Polymers 45, 183–188.
Dalmas, F., Cavaillé, J.Y., Gauthier, C., Chazeau, L., Dendievel, R., 2007. Viscoelastic behavior and electrical properties of flexible nanofiber filled polymer nanocomposites. Influence of processing conditions. Composites Science and Technology 67, 829–839.
degree Well, S.E., Renneckar, P., Esker, A.R., Heinze, T., Gate-Holm, P., Vaca-Garcia, C., 2004. Surface modification of cellulose fibers: towards wood composites by biomimetics. Comptes Rendus Biologies 327, 945–953.
Dubief, D., Samain, E., Dufresne, A., 1999. Polysaccharide microcrystals reinforced amorphous poly(b-hydroxyoctanoate) nanocomposite materials. Macromolecules 32 (18), 5765–5771.
Dufresne, A., Vignon, M.R., 1998. Improvement of starch film performances using cellulose microfibrils. Macromolecules 31, 2693–2696.
Dufresne, A., Dupeyre, D., Vignon, M.R., 2000. Cellulose microfibrils from potato tuber cells: processing and characterization of starch–cellulose microfibril composites. Journal of Applied Polymer Science 76 (14), 2080–2092.
Gennadios, A., 2002. Protein-based Films and Coatings. CRC Press, Boca Raton, USA. p. 646.
Ibrahim, M.M., El-Zawawy, W.K., Nassar, M.A., 2010. Synthesis and characterization of polyvinyl alcohol/nanospherical cellulose particle films. Carbohydrate Polymers 79, 694–699.
Irissin-Mangata, J., Bauduin, G., Boutevin, B., Gontard, N., 2001. New plasticizers for wheat gluten films. European Polymer Journal 37, 1533.
Jayaramudu, J., Jeevan, D., Reddy, P., Guduri1, B.R., Varada, A., 2009. Properties of natural fabric polyalthia cerasoides. Fibers and Polymers 10 (3), 338–342.
Jordan, J., Jacob, K.I., Tannenbaum, R., Sharaf, M.A., Jasiuk, I., 2005. Experimental trends in polymer nanocomposites: a review. Materials Science and Engineering A 393 (1–2), 1–11.
Kahn, J., 2006. Nano's big future – tiny technology promises big rewards. Some may already be in your closet. National Geographic 209, 98–119.
Kim, Y.T., 2005. Development and Characterization of Gelatin Film as Active Packaging Layer. Clemson University, Clemson.
Klem, D., Heublein, B., Fink, H., Bohn, A., 2005. Cellulose: fascinating biopolymer and sustainable raw material. Angewandte Chemie (International Edition) 44, 3358–3393.
Klemm, D., Schmauder, H.-P., Heinze, T., 2002. Cellulose. In: Vandamme, E., De Baets, A., Steinbüchel, A. (Eds.), Biopolymers: Biology, Chemistry, Biotechnology, Applications, vol. 6. Wiley-VCH, Weinheim, pp. 275–319.
Krochta, J.M., Miller, K.S., 1997. Oxygen and aroma barrier properties of edible films: a review. Trends in Food Science and Technology 8, 228–237.
Lagaron, J.M., Catalá, R., Gavara, R., 2004. Structural characteristics defining high barrier polymeric materials. Materials Science and Technology 20, 1–7.
Lieberman, E.R., Gilbert, S.G., 1973. Gas permeation of collagen films as affected by cross-linkage, moisture, and plasticizer content. Journal of Polymer Science 41, 33–43.
Liu, D.Y., Yuan, X.W., Bhattacharyya, D., Easteal, A.J., 2010. Characterization of solution cast cellulose nanofibre–reinforced poly(lactic acid). Express Polymer Letters 4 (1), 26–31.
Lu, Y., Weng, L., Cao, X., 2005. Biocomposites of plasticizes starch reinforced with cellulose crystallites from cottonseed linter. Macromolecular Bioscience 5, 1101–1107.
Ludueña, L.N., Alvarez, V.A., Vasquez, A., 2007. Processing and microstructure of PCL/clay nanocomposites. Materials Science and Engineering: A, 121–129.
Marcovich, N.E., Reboredo, M.M., Aranguren, M.I., 1996. FTIR spectroscopy applied to woodflour. Composite Interfaces 4 (3), 119–132.
Marcovich, N.E., Reboredo, M.M., Aranguren, M.I., 1999. Moisture diffusion in polyester–woodflour composites. Polymer 40 (26), 7313–7320.
Marcovich, N.E., Bellesi, N.E., Auad, M.L., Nutt, S.R., Aranguren, M.I., 2006. Cellulose micro/nanocrystals reinforced polyurethane. Journal of Materials Research 21 (4), 870–881.
Mathew, A.P., Dufresne, A., 2002. Morphological investigation of nanocomposites from sorbitol plasticized starch and tunicin whiskers. Biomacromolecules 3 (3), 609–617.
Monedero, F.M., Fabra, M.J., Talens, P., Chiralt, A., 2009. Effect of oleic acid–beeswax mixtures on mechanical, optical and water barrier properties of soy protein isolate based films. Journal of Food Engineering 91, 509–515.
Müller, C.M.O., Borges Laurindo, J., 2009. Effect of cellulose fibers on the crystallinity and mechanical properties of starch-based films at different relative humidity values. Carbohydrate Polymers 77, 293–299.
Müller, C.M.O., Borges Laurindo, J., Yamashita, F., 2009. Effect of cellulose fibers addition on the mechanical properties and water vapor barrier of starch-based films. Food Hydrocolloids 23, 1328–1333.
Oksman, K., Mathew, A.P., Bondeson, D., Kvien, I., 2006. Manufacturing process of cellulose whiskers/polylactic acid nanocomposites. Composites Science and Technology 66, 2776–2784.
Paralikar, S.A., Simonsen, J., Lombardi, J., 2008. Poly(vinyl alcohol)/cellulose nanocrystal barrier membranes. Journal of Membrane Science 320 (1–2), 248–258.
Park, H.J., 1991. Edible Coating for Fruits and Vegetables: Determination of Gas Diffusivities, Prediction of Internal Gas Composition and Effects of the Coating on Shelf Life. University of Georgia, Athens. pp. 23–30.

Please cite this article in press as: Pereda, M., et al. Structure and properties of nanocomposite films based on sodium caseinate and nanocellulose fibers. Journal of Food Engineering (2010), doi:10.1016/j.jfoodeng.2010.10.001

Pereda, M., Aranguren, M.I., Marcovich, N.E., 2008. Characterization of chitosan/caseinate films. Journal of Applied Polymer Science 107 (2), 1080–1090.

Pereda, M., Aranguren, M.I., Marcovich, N.E., 2009. Water vapor absorption and permeability of films based on chitosan and sodium caseinate. Journal of Applied Polymer Science 111 (6), 2777–2784.

Pereda, M., Aranguren, M.I., Marcovich, N.E., 2010. Effect of crosslinking on the properties of sodium caseinate films. Journal of Applied Polymer Science 116 (1), 18–26.

Pérez, O.E., Carrera Sánchez, C., Pilosof, A.M.R., Rodríguez Patino, J.M., 2009. Kinetics of adsorption of whey proteins and hydroxypropyl-methyl-cellulose mixtures at the air–water interface. Journal of Colloid and Interface Science 336, 485–496.

Petersson, L., Oksman, K., 2006. Biopolymer based nanocomposites: comparing layered silicates and microcrystalline cellulose as nanoreinforcement. Composites Science and Technology 66, 2187–2196.

Prodpran, T., Benjaku, S., Artharn, A., 2007. Properties and microstructure of protein-based film from round scad (*Decapterus maruadsi*) muscle as affected by palm oil and chitosan incorporation. International Journal of Biological Macromolecules 41, 605–614.

Psomiadou, E., Arvanitoyannis, I., Yamamoto, N., 1996. Edible films made from natural resources; microcrystalline cellulose (MCC), methylcellulose (MC) and corn starch and polyols – part 2. Carbohydrate Polymers 31, 193–204.

Qiao, R., Brinson, L.C., 2009. Simulation of interphase percolation and gradients in polymer nanocomposites. Composites Science and Technology 69 (3–4), 491–499.

Ragauskas, A.J., Williams, C.K., Davison, B.H., Britovsek, G., Cairney, J., Eckert, C.A., Frederick, W.J., Hallett, J.P., Leak, D.J., Liotta, C.L., Mielenz, J.R., Murphy, R., Templer, R., Tschaplinski, T., 2006. The path forward for biofuels and biomaterials. Science 311, 484–489.

Samir, M.A.S.A., Alloin, F., Dufresne, A., 2005. Review of recent research into cellulosic whiskers, their properties and their application in nanocomposites field. Biomacromolecules 6, 612–626.

Sanchez-Garcia, M.D., Gimenez, E., Lagaron, J.M., 2008. Morphology and barrier properties of solvent cast composites of thermoplastic biopolymers and purified cellulose fibers. Carbohydrate Polymers 71, 235–244.

Sothornvit, R., Krochta, J.M., 2001. Plasticizer effect on mechanical properties of β-lactoglobulin films. Journal of Food Engineering 50, 149–155.

Su, J.-F., Huang, Z., Yuan, X.-Y., Wang, X.-Y., Li, M., 2010. Structure and properties of carboxymethyl cellulose/soy protein isolate blend edible films crosslinked by Maillard reactions. Carbohydrate Polymers 79, 145–153.

Svagan, A.J.Ç., Hedenqvist, M.S., Berglund, L., 2009. Reduced water vapour sorption in cellulose nanocomposites with starch matrix. Composites Science and Technology 69 (3–4), 500–506.

Tharanathan, R.N., 2003. Biodegradable films and composite coatings: past, present and future. Trends in Food Science and Technology 14 (3), 71–78.

Tunç, S., Duman, O., 2010. Preparation and characterization of biodegradable methyl cellulose/montmorillonite nanocomposite films. Applied Clay Science 48, 414–424.

Villalobos, R., Chanona, J., Hernández, P., Gutiérrez, G., Chiralt, A., 2005. Gloss and transparency of hydroxypropyl methylcellulose films containing surfactants as affected by their microstructure. Food Hydrocolloids 19 (1), 53–61.

Wang, L.Z., Liu, L., Holmes, J., Huang, J., Kerry, J.F., Kerry, J.P., 2008. Effect of pH and addition of corn oil on the properties of whey protein isolate-based films using response surface methodology. International Journal of Food Science and Technology 43 (5), 787–796.

Yang, L., Paulson, A.T., 2000. Effects of lipids on mechanical and moisture barrier properties of edible gellan film. Food Research International 33, 571–578.

Please cite this article in press as: Pereda, M., et al. Structure and properties of nanocomposite films based on sodium caseinate and nanocellulose fibers. Journal of Food Engineering (2010), doi:10.1016/j.jfoodeng.2010.10.001